Korean J. Chem. Eng., 37(1), 176-183 (2020)
DOI: 10.1007/s11814-019-0432-6

pISSN: 0256-1115
eISSN: 1975-7220

Carbon supported palladium-copper bimetallic catalysts for promoting electrochemical oxidation of formic acid and its utilization in direct formic acid fuel cells

Jongwon Yang*, Seungwon Yang*, Yongjin Chung, and Yongchai Kwon*,†**

*Graduate school of Energy and Environment, Seoul National University of Science and Technology, 232 Gongneung-ro, Nowon-gu, Seoul 01811, Korea
**Department of Chemical and Biological Engineering, Korea National University of Transportation, 50 Daehak-ro, Chungju, Chungbuk 27469, Korea
(*Received 14 September 2019 • accepted 14 November 2019*)

Abstract−Carbon supported palladium-copper (Pd-Cu) bimetallic catalysts (Pd_xCu_y/Cs) are fabricated by modified polyol method to enhance the reaction rate of formic acid oxidation reaction (FAOR) and the performance of direct formic acid fuel cell (DFAFC) through weakening the bond with the intermediate of formic acid. According to the evaluations, when the ratio of Pd and Cu is 3 : 1 (Pd_3Cu_1/C), catalytic activity is best. Its maximum current density is 1.68-times better than that of commercial Pd/C. Even from the optical and spectroscopic characterizations, such as TEM, EDS, XPS and XRD, Pd_3Cu_1/C shows an optimal particle size and a higher degree of alloying. This is because in Pd_3Cu_1/C catalyst, the d-band center that induces the weakening in adsorption of formate anion groups to Pd surface is most positively shifted, and this positive shift promotes the reaction rate of FAOR, which is the rate determining step. When the performance of DFAFCs using the Pd_xCu_y/C catalysts is measured, the maximum power density (MPD) of DFAFC using Pd_3Cu_1/C catalyst is 158 mW cm^{-2}, and this is the best MPD compared to that of DFAFCs using other Pd_xCu_y/C catalysts. In addition, in a comparison with commercial Pd/C catalyst, when the same amount of catalyst is loaded, MPD of DFAFC using Pd_3Cu_1/C catalyst is 22.5% higher than that of DFAFC using commercial Pd/C.

Keywords: Direct Formic Acid Fuel Cell (DFAFC), Formic Acid Oxidation Reaction (FAOR), PdCu Bimetallic Catalyst, Modified Polyol Method, Center of d-Band

INTRODUCTION

There have been many demands for developing highly efficient and long-lasting fuel cell systems, replacing rechargeable batteries used as the power supply system for the operation of electronic devices [1-7]. As an alternative, in the early stage, polymer electrolyte membrane fuel cells (PEMFC) received deep attention. PEMFC uses hydrogen as fuel, and the hydrogen gas has favorable attributes like clean property and fast reaction rate [8-12]. Despite that, hydrogen gas explodes relatively easily, and thus the security issue that is related to the safe control of hydrogen fuel has been a continuous concern. To avoid the concerns and guarantee its proper storage and utilization capabilities, the hydrogen fuel should be tightly sealed, and to do the tight sealing, much expense should be needed [13-16].

To overcome the difficulty of reserving the hydrogen fuel in the PEMFC, direct formic acid fuel cell (DFAFC) that uses a less explosive formic acid as the fuel has been suggested [17-20]. Because the formic acid exists as a liquid state at atmosphere, its stability is excellent. In addition, there are other important merits related to formic acid fuel [21-23]. First, it is not toxic to the human body and thus it is used as food additive. Second, its easy dissociation into proton and formate anion in aqueous solution makes the use of formic acid as electrolyte possible, and third, the crossover rate of formic acid is relatively low because of the repulsive force between formate anions and ion clusters, increasing the degree of freedom for selecting membrane. Moreover, the conversion efficiency of DFAFC is expected as 106%, while that in PEMFC is less than 90% [19,21].

However, formic acid fuel shows low energy density and its reaction mechanism is not fully elucidated yet. Most of all, understanding the reaction mechanism of formic acid oxidation reaction (FAOR) and improving its reaction rate are very important because the reaction depends on the performance of DFAFC. Thus, to date, there have been various attempts to elucidate the reaction mechanism, increasing the reaction rate of FAOR [21,22,24-26].

To increase the reaction rate of FAOR, appropriate catalysts are required, and for that purpose Pt has been mainly considered [28, 29]. However, its easy CO-poisoning, expensive cost and localization of the Pt reserves prevented its utilization as the catalyst. As an alternative, Pd was introduced because of its less CO poisoning property [9,30,31]. However, even Pd has still wonder about the durability for FAOR, while its price is also rapidly surging. To mitigate the problems of Pd, PdM bimetallic catalysts consisting of Pd and cheap transition metals, such as PdAg, PdAu, PdFe, PdNi and PdCo, were suggested due to their own unique benefit [32-37]. In this study, we focus on Pd_xCu_y bimetallic catalyst because Cu can increase the interval between d-band center and fermi energy, and

†To whom correspondence should be addressed.
E-mail: kwony@seoultech.ac.kr

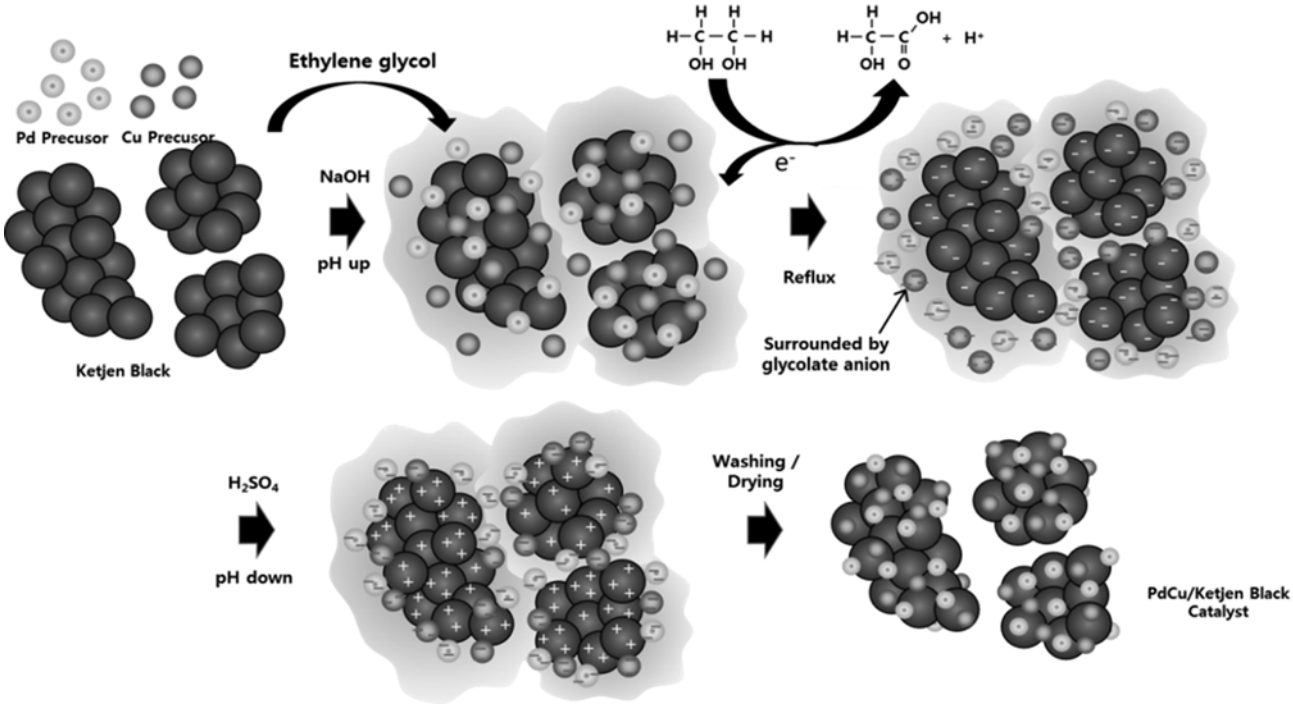

Fig. 1. Synthetic procedure of Pd_xCu_y/C catalysts fabricated by modified-polyol method.

such increased interval can facilitate (i) a facile absorption/desorption of formic acid atoms, and (ii) the activity of FAOR, while overall cost needed for synthesizing the catalyst is saved due to the utilization of cheap Cu metal.

Here, Pd is alloyed with transition metal, Cu, using modified polyol method, and as a result, carbon supported bimetallic catalyst (Pd_xCu_y/C) is fabricated [38,39]. After the Pd_xCu_y/C catalysts are formed, the optimal precursor ratio of Pd to Cu is determined by evaluating their catalytic activity for FAOR. In terms of the optical and spectroscopic characterizations, analysis using equipment such as transmission electron microscopy (TEM), X-ray photoelectron spectroscopy (XPS), X-ray diffraction (XRD), energy dispersive spectrometer (EDS) are implemented to examine the microstructure of Pd_xCu_y/C. Furthermore, electrochemical characterizations, such as cyclic voltammetry (CV) and polarization curve are considered to quantify the activity for FAOR of all the catalysts and the performance of DFAFCs using the catalysts. With the results, Pd_3Cu_1/C catalyst showing an excellent catalytic activity for FAOR and the best performance of DFAFC is decided as the best one. Indeed, these results will be a milestone to achieve consolidated protocol about FAOR and DFAFC.

EXPERIMENTAL

1. Materials

Ketjen black EC 600JD was purchased from Lion Corporation (Tokyo, Japan), Ethylene glycol, 99.5%, Palladium(II) chloride ($PdCl_2$, 99.0%), Sodium hydroxide, bead (NaOH, 98.0%), Copper(II) chloride dehydrate ($CuCl_2$, 99.0%) and hydrogen peroxide(H_2O_2, 30%) were purchased from Samchun Pure Chemical (Gyeonggi, Korea). Sulfuric acid (H_2SO_4, 97%) was purchased from Matsunoen Chemicals (OSAKA, Japan), Nafion 117 membrane was purchased from Dupon, Platinum on carbon (Pt/C, 40 wt%) was purchased from Sigma Aldrich(Milwaukee, WI, USA).

2. Synthesis Procedure of Carbon Supported PdCu Bimetallic Catalysts

The carbon supported PdCu bimetallic catalyst (Pd_xCu_y/C) was synthesized by modified-polyol method, controlling the atomic ratio of Pd and Cu. The metal content of catalyst was fixed to 40 wt%. A schematic illustration about Pd_xCu_y/C catalyst synthesis process is introduced in Fig. 1 [38,39].

For synthesizing Pd_xCu_y/C catalysts, the predetermined amounts of $PdCl_2$ and $CuCl_2$ precursors were dissolved into 240 mL ethylene glycol to form mixed solution, and the mixed solution was stirred for 30 min. 75 mg of carbon supporter (Ketjen black EC 600JD) was then inserted to the mixed solution with stirring for 30 min. After that, 0.1 M NaOH was added until the pH of mixed solution reached 11. After mixing process, it was refluxed at 160 °C for 3 h. During this reflux step, ethylene glycol is oxidized and by the reaction, the metal precursor is changed into the micelles, producing the particles of nano size. After reflux step, the mixed solution was stirred for 12 h for stabilization. Then, this was titrated with 0.5 M H_2SO_4 until pH reached 3. By this titration, the polarity of reduced metal particles and carbon supporters is differentiated. When their zeta potentials were measured, that of nanoparticles had positive values, while that of carbon supporters had negative values. Due to the opposite zeta potentials between metal nanoparticles and carbon supporters, electrostatic attractive force is applied. Then, the mixed solution was filtered to separate Pd_xCu_y/C from remaining solution. The Pd_xCu_y/C was then dried at 120 °C for 12 h in vacuum oven. Finally, the powders of Pd_xCu_y/C catalyst were produced.

3. Optical Characterizations

The particle size and the degree of dispersion of commercial Pd/C and Pd_xCu_y/C catalysts were optically characterized by transmission electron microscopy (TEM, JEM-1011, JEOL LTD). In addition, energy dispersive spectroscopy (EDS) analysis was performed to measure the individual phase of Pd, Cu and carbon. The phase matching and pattern analysis of all the catalysts were also characterized by X-ray powder diffraction (XRD, X'PERT diffractometer of Philips with CuKα radiation). [38] The 2θ range for XRD measurements was 35-80° and they were measured at 40 kV and 15 mA at room temperature with the interval of 0.01°. X-ray photoelectron spectroscopy (XPS, ESCA LAB250, VG Scientific) analysis was performed to measure the valance band of Pd_xCu_y/C and commercial Pd/C catalysts. The center of the d-bend is estimated by density functional theory.

4. Electrochemical Measurements

Electrochemical measurements were carried out using potentiostat (CHI 7200, CH instrument, USA). For the electrochemical measurements like cyclic voltammetry (CV), and rotating disk electrode (RDE) were prepared working electrode. To fabricate working electrode, catalytic powder was mixed with deionized (DI) water, isopropanol l(IPA) and 5 wt% Nafion solution under sonication for 10 min. After mixing, the catalytic slurry was dropped on glass carbon disk electrode (GCE). Pt wire and Ag/AgCl soaked in 3 M NaCl were used as counter and reference electrodes. 0.5 M H_2SO_4 was used as an electrolyte. When FAOR was measured, an additional 0.5 M formic acid solution was added and mixed [38].

For DFAFC single cell tests, membrane electrode assemblies (MEAs) with active area of 9.0 cm^2 were prepared. Pt/C was introduced as cathodic catalyst, while the corresponding Pd and PdBi based catalysts were assigned as anodic catalysts, respectively. The catalyst powders were ultrasonically mixed with 5% Nafion solution, DI water and IPA for the preparation of catalyst ink. For fabricating MEA, CCM (catalyst coated membrane) method was used. Nafion 117 (Dupont) was used as membrane to reduce the crossover of formic acid molecules. The corresponding catalyst inks were directly air-sprayed onto both sides of the membrane. The loading amount was 1.2 mg cm^{-2} for anodic catalyst and 0.8 mg cm^{-2} for cathodic catalyst, respectively [38]. The MEA was then assembled with gas diffusion layers (GDL, cathode side, E-Tek division) and gasket (TF 350, CNL, Inc.). The completed MEAs were then placed between two graphite plates that had the engraved serpentine flow channels. After the single cell was assembled, it was installed at a fuel cell test station (Fuel Cell Control System, CNL Inc.) for DFAFC tests. While the DFAFC single cell test, cell temperature was maintained as 65 °C, while for cathode, air was supplied at a rate of 800 cc min^{-1}. In anode, 3.0 M formic acid was fed at a rate of 10 cc min^{-1} [38].

RESULTS AND DISCUSSION

1. Electrochemical Characterizations

It is crucial to investigate the electrochemical behaviour of catalysts prepared by modified polyol method for predicting their catalytic activity. To that end, CV curves of Pd_xCu_y/C and commercial Pd/C catalysts were measured under N_2 purged state (Fig. 2). Ac-

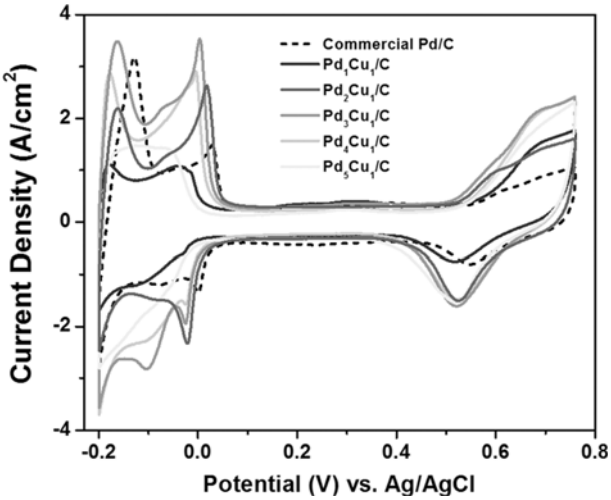

Fig. 2. The CV curves of Pd/C (dashed line) and Pd_xCu_y/C (solid lines) catalysts that are loaded on GCE in 0.5 M H_2SO_4 solution with a scan rate of 20 mVs^{-1}.

cording to Fig. 2, all the catalysts showed significant anodic reaction peaks at −0.2 (hydrogen reaction catalyzed by Pd(111)), 0 (hydrogen reaction catalyzed by Pd(100) and 0.5 V (Pd-oxide reaction) (vs. Ag/AgCl), while their peak intensity was clearly different depending on the ratio of Pd to Cu precursors. This indicates that the catalytic activity of the catalysts varied by the precursor ratio, although Pd_xCu_y/C and commercial Pd/C catalysts may have similar crystalline and oxide structure to react with formic acid that was proved by the similar reaction peak potentials of CV curves.

To confirm the effect of precursor ratio of Pd to Cu on the reaction rate of FAOR, the CVs of commercial Pd/C and Pd_xCu_y/C catalysts were measured with 0.5 M formic acid that is dissolved into 0.5 M H_2SO_4 (Fig. 3). As shown in Fig. 3, the maximum current density of commercial Pd/C, Pd_1Cu_1/C, Pd_2Cu_1/C, Pd_3Cu_1/C, Pd_4Cu_1/C and Pd_5Cu_1/C was 64.97, 55.15, 98.82, 109.17, 67.80 and 39.80 mA cm^{-2}, respectively. It indicates that the alloying of Pd and

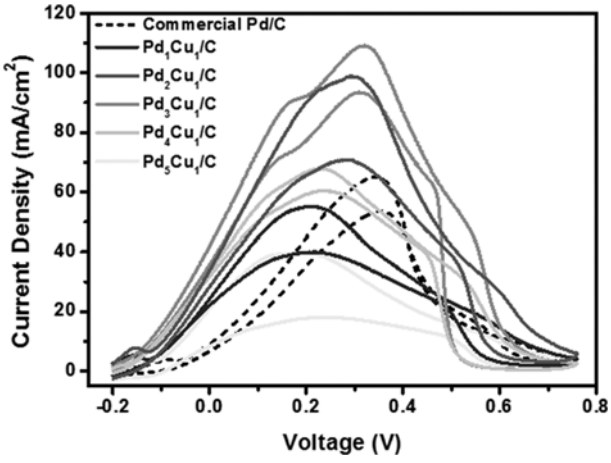

Fig. 3. The CV curves of Pd/C (dashed line) and Pd_xCu_y/C (solid lines) catalysts that are loaded on GCE in 0.5 M H_2SO_4+ 0.5 M HCOOH solution with a scan rate of 20 mVs^{-1}.

Cu, and the precursor ratio between Pd and Cu affect the reaction rate of FAOR. It is due to the absorption energy of formate anion groups (COOH) absorbed to the Pd surface, which can be varied by the concentration of additional metal [40,41]. Namely, the absorption energy of COOH absorbed to Pd surface is dependent on the precursor ratio of Pd to Cu because the different Pd-Cu bimetallic structure can form different charge depletion state on Pd, which induces a change in absorption energy of Pd for absorbed chemical species by the adoption of another metal component. Owing to that, the catalytic reaction can be enhanced by facile absorption/desorption of COOH molecules [37,42]. However, the increase in catalytic activity was not proportional to the increase of Cu atoms because an excessive amount of Cu atoms may lead to an incomplete Pd-Cu alloy or very low absorption energy.

Fig. 3 also supports the above hypothesis. When the concentrations of Cu precursor were low (Pd_5Cu_1/C, Pd_4Cu_1/C and Pd_3Cu_1/C), the reaction rate of FAOR, that is expressed as maximum current density, increased. In contrast, when the concentrations of Cu precursor were high (Pd_2Cu_1/C and Pd_1Cu_1/C), the maximum current density for FAOR was reduced.

Based on that, this was recognized that (i) there are pros and cons regarding the reaction rate of FAOR when Cu alloying is considered, and (ii) in the catalyst consisting of the optimal Pd to Cu precursor ratio of 3 : 1 (Pd_3Cu_1/C), the reaction rate of FAOR is 1.68 times better than that produced by commercial Pd/C catalyst.

2. Optical Characterizations Using TEM-EDS of the Corresponding Catalysts

For optically investigating how modified polyol method affects the structural property of Pd_xCu_y/C catalysts, HR-TEM and EDS analysis of Pd_xCu_y/C catalysts was carried out. As a control sample, the analysis of commercial Pd/C catalyst was also implemented (Figs. 4 and 5). As shown in Fig. 4, Pd_5Cu_1/C and Pd_4Cu_1/C catalysts (catalysts fabricated by low Cu precursor ratios) showed relatively large spherical metal clusters, while Pd_2Cu_1/C and Pd_1Cu_1/C catalysts (catalysts fabricated by high Cu precursor ratios) showed small metal nanoparticles, which were well dispersed. Fig. 5 shows the particle size distribution of catalysts. According to Fig. 5, the average particle size of commercial Pd/C, Pd_1Cu_1/C, Pd_2Cu_1/C, Pd_3Cu_1/C, Pd_4Cu_1/C and Pd_5Cu_1/C catalysts was 4.30, 3.51, 3.69, 4.26, 4.59 and 4.64 nm, demonstrating that the particle size was curtailed as the concentration of Cu precursor increased. Interestingly, the average particle size of Pd_3Cu_1/C (4.26 nm) was very similar to that of commercial Pd/C (4.3 nm), and this similar particle size between Pd_3Cu_1/C and commercial Pd/C catalysts may have induced a similar reaction rate for FAOR. This is also supported by the previously reported result [43]. According to the report, in Pd based catalysts, the catalytic activity for FAOR is dependent on its particle size [43].

Moreover, for evaluating the relationship between electrochemical performance and chemical composition, identifying the atomic ratio of the prepared catalysts is important [37,44]. To do that, TEM-EDS analysis was carried out and the results summarized in Table 1. According to the analysis, the metal ratios of Pd to Cu

Table 1. The portion of each component of the Pd_xCu_y/C catalysts determined by TEM/EDS

Samples (Pd_xCu_y/C)	Composition			
	Weight %			Atomic ratio
	Pd	Cu	C	Pd : Cu
Pd_1Cu_1/C	20.1	18.8	61.1	1 : 1.53
Pd_2Cu_1/C	21.9	17.6	60.5	1 : 1.31
Pd_3Cu_1/C	25.3	14.7	60	1.02 : 1
Pd_4Cu_1/C	26.4	14.3	59.3	1.10 : 1
Pd_5Cu_1/C	27.1	14.9	58	1.06 : 1

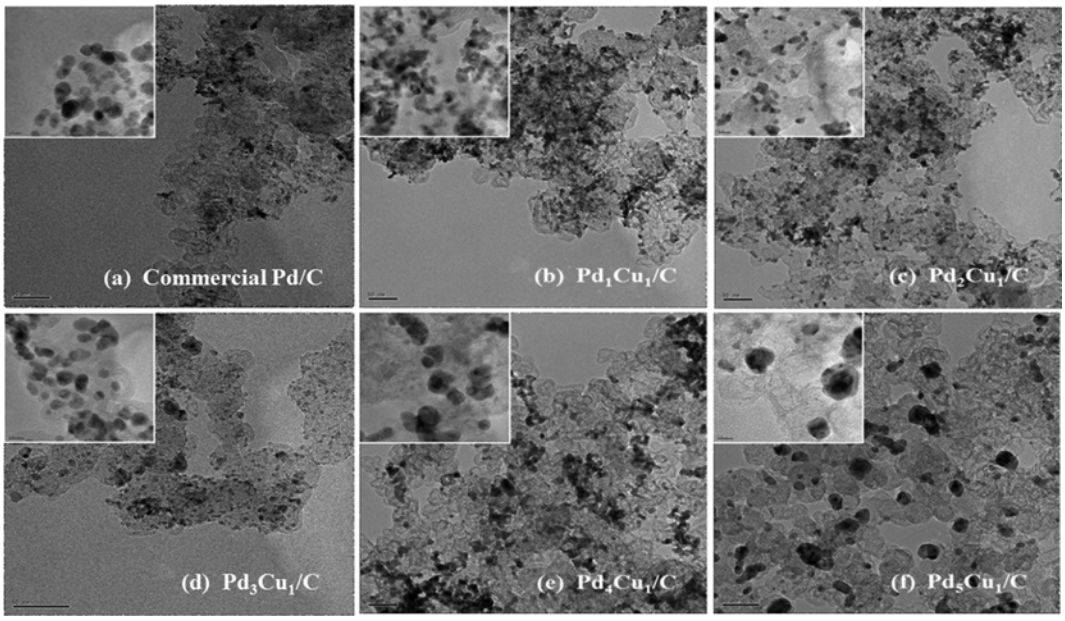

Fig. 4. HRTEM images of (a) commercial Pd/C, (b) Pd_1Cu_1/C, (c) Pd_2Cu_1/C (d) Pd_3Cu_1/C, (e) Pd_4Cu_1/C and (f) Pd_5Cu_1/C catalysts. The scale bar represents 50 nm.

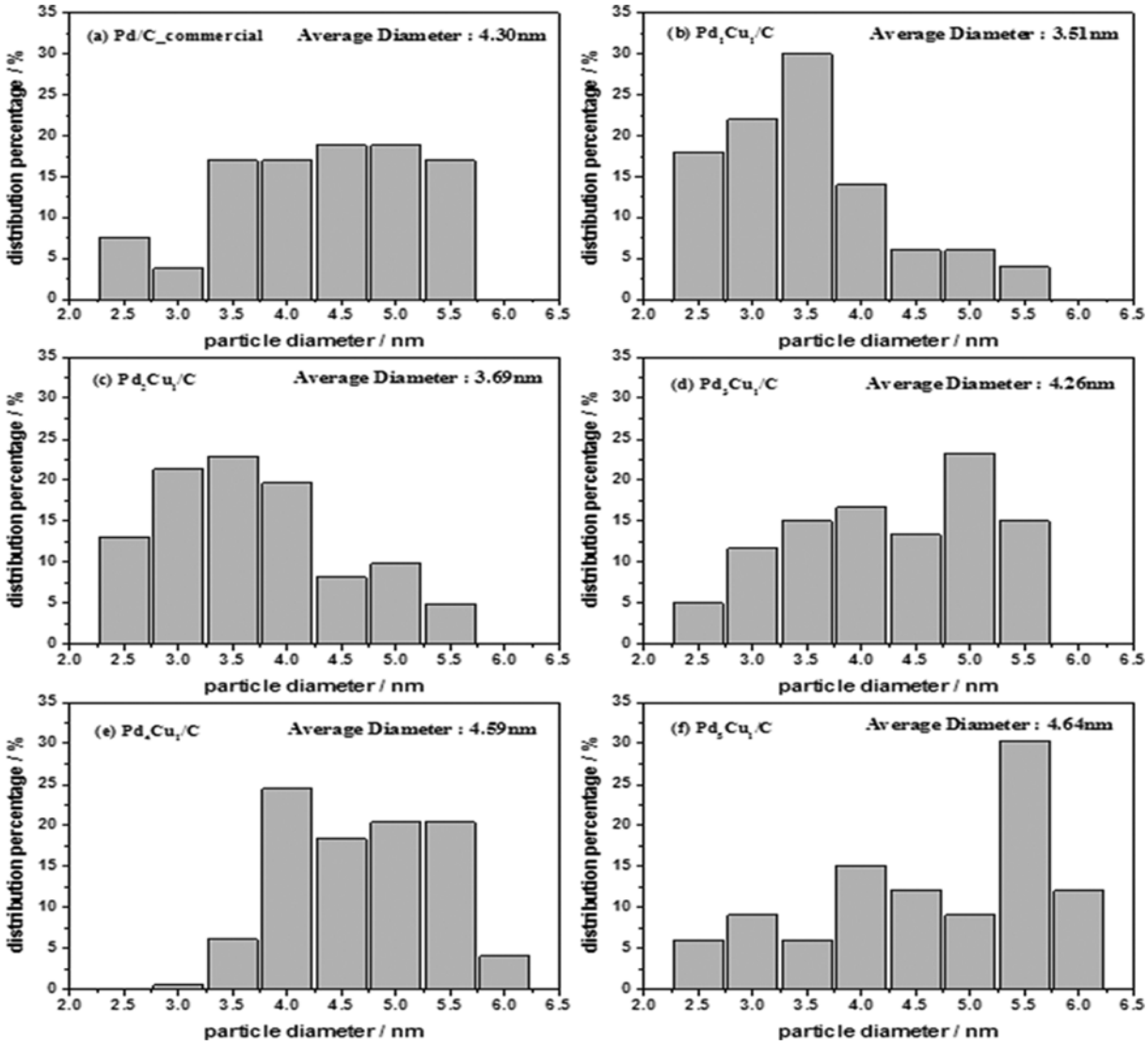

Fig. 5. Particle-size distribution of (a) commercial Pd/C, (b) Pd_1Cu_1/C, (c) Pd_2Cu_1/C, (d) Pd_3Cu_1/C, (e) Pd_4Cu_1/C and (f) Pd_5Cu_1/C catalysts.

increased as the concentration of Cu precursor decreased when the portion of Cu precursor was high (Pd_1Cu_1/C, Pd_2Cu_1/C and Pd_3Cu_1/C). In contrast, when the portion of Cu precursor was low (Pd_4Cu_1/C and Pd_5Cu_1/C), the opposite result was observed. This indicates the atomic ratio of Pd to Cu was almost preserved as 1 : 1 even though the Pd precursor was more included, such as Pd_4Cu_1/C and Pd_5Cu_1/C, during the modified polyol process, and there are other important factors that affect the catalytic activity of FAOR besides the atomic ratio between Pd and Cu.

3. Spectroscopic Characterizations Using XPS and XPD of the Corresponding Catalysts

To evaluate the effect of bimetallic structure on the reaction rate of FAOR spectroscopically, XPS analysis was conducted (Fig. 6 and Table 2). As shown in Table 2, the $Pd3d_{5/2}$ binding energy (BE) of Pd_1Cu_1/C and Pd_3Cu_1/C catalysts was the same as 355.200 eV, while that of the others was 355.181 eV. It indicates that Pd_1Cu_1/C and Pd_3Cu_1/C catalysts have more bimetallic alloy structure than the others because the positive shift of BE on $Pd3d_{5/2}$ shows a stronger binding energy due to the electron transfer from Pd to Cu [37, 42]. Moreover, the sum of Pd-O ratio in $Pd3d_{5/2}$ and $Pd3d_{3/2}$ peaks was also high in Pd_1Cu_1/C and Pd_3Cu_1/C catalysts, confirming that Pd_3Cu_1/C catalyst has more Pd-Cu alloying structure [37,42]. This interpretation is important because the degree of alloying is dependent on the absorption energy of COOH as explained in Fig. 3, and thus a high degree of alloying and a high Pd concentration in Pd_xCu_y will lead to a better reaction rate for FAOR.

For investigating the alloying effect and confirming the above assumption, the average d-band center (μ_p) was assessed from XPS valence band that was previously reported by Ha group [37] (Fig. 7). To estimate the average μ_p of Pd_xCu_y/C catalysts, the value measured from commercial Pd/C was considered as the standard one. As shown in Fig. 7, the μ_p of Pd_1Cu_1/C, Pd_2Cu_1/C, Pd_3Cu_1/C, Pd_4Cu_1/C and Pd_5Cu_1/C were 3.5998, 3.5884, 3.5934, 3.587 and 3.5857 eV, respectively. It is well known that the positive shift of μ_p induces a weakening in adsorption of COOH into Pd surface, enhancing the reaction rate of FAOR. This is because the weakening in ad-

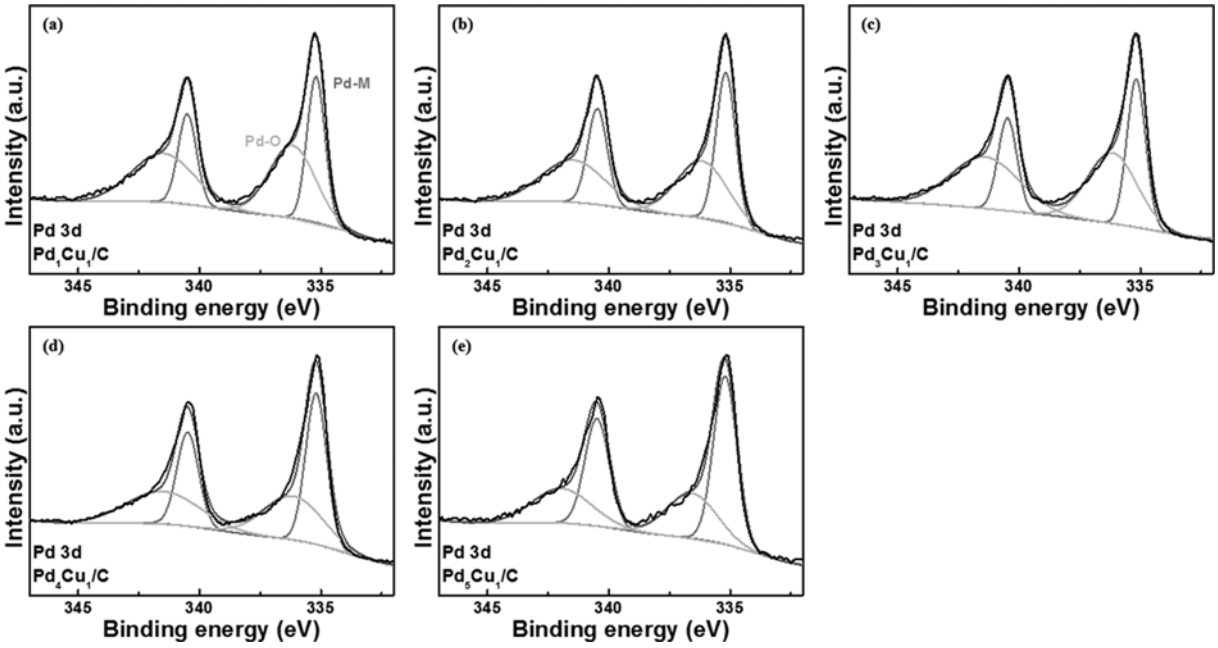

Fig. 6. Pd3d analysis of (a) Pd_1Cu_1/C, (b) Pd_2Cu_1/C, (c) Pd_3Cu_1/C, (d) Pd_4Cu_1/C and (e)Pd_5Cu_1/C catalysts that was measured by XPS.

Table 2. Binding energy of $Pd3d_{5/2}$ and $Pd3d_{3/2}$ peaks of the Pd_xCu_y/C catalysts determined by XPS

Samples	Pd3d		Area percentage in Pd3d	
	Pd-M (eV)	Pd-O (eV)	Pd-M (%)	Pd-O (%)
Pd_1Cu_1/C	335.200	340.506	40.33	59.67
Pd_2Cu_1/C	335.182	340.476	46.22	53.78
Pd_3Cu_1/C	335.200	340.487	39.28	60.72
Pd_4Cu_1/C	335.181	340.474	51.67	48.33
Pd_5Cu_1/C	335.180	340.469	48.59	51.41

sorption of COOH accelerates the desorption of oxygen (O) atoms, which is supposed to determine the reaction rate of FAOR [40,41]. When this theory is adopted, the μ_p of Pd_1Cu_1/C and Pd_3Cu_1/C was significantly shifted positively than the others, and this means that Pd_1Cu_1/C and Pd_3Cu_1/C are more close to Pd-Cu alloying structure than the others. This result is well matched with the results shown in Table 2 and Fig. 6, confirming again that Pd_3Cu_1/C catalyst is the optimal one to enable a high degree of desirable bimetallic alloying structure, and the excellent reaction rate of FAOR is induced by this property of Pd_3Cu_1/C catalyst.

Next, XRD analysis was conducted to identify the effect of precursor ratio on the microstructure of Pd (Fig. 8). According to Fig. 8, the catalysts prepared by a high Cu precursor ratio (Pd_1Cu_1/C, Pd_2Cu_1/C and Pd_3Cu_1/C) showed Pd (111) peak at 40.21° of 2θ. In contrast, the peak in Pd_4Cu_1/C and Pd_5Cu_1/C was shown in 40.12°. Meanwhile, that of commercial Pd/C was 40.08°. These results are similar to previously reported results that suggest a high concentration of Cu atom causes the increase of 2θ, which means that lattice structure is deformed due to the Cu atoms [37,42,44]. This demonstrates that the degree of alloying was high as the ratio of Cu precursor increased, although the lattice structure of all five

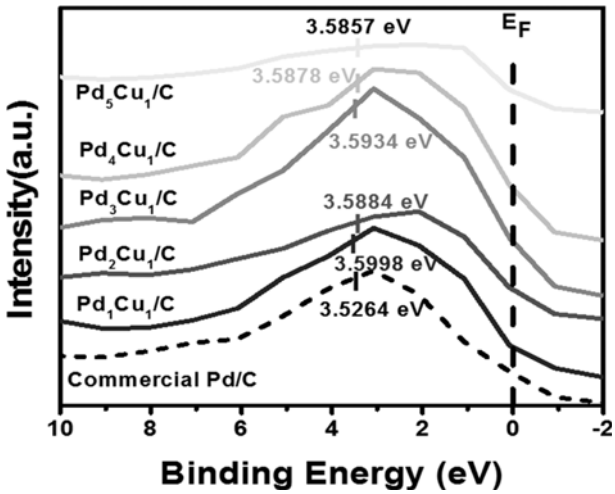

Fig. 7. The difference between d-bond and Fermi energy band of commercial Pd/C and Pd_xCu_y/C catalysts that are measured by XPS.

catalysts was deformed by Pd-Cu alloying.

Taken together, through the TEM, EDS, XPS and XRD analysis, it is determined that Pd_3Cu_1/C has not only a relatively high Pd atom concentration but also a high degree of alloying despite relatively lower Cu precursor ratio, and such unique microstructure contributed to the enhancement in the reaction rate for FAOR.

4. Polarization Curves of DFAFCs Using Commercial Pd/C and Pd_xCu_y/C Catalysts

Lastly, the polarization curves of DFAFCs using Pd_xCu_y/C as anodic catalyst were measured and compared with that using commercial Pd/C (Fig. 9). As shown in Fig. 9, maximum power density (MPD) of DFAFCs using commercial Pd/C, Pd_1Cu_1/C, Pd_2Cu_1/C, Pd_3Cu_1/C, Pd_4Cu_1/C and Pd_5Cu_1/C was 129, 112, 142, 158, 121 and

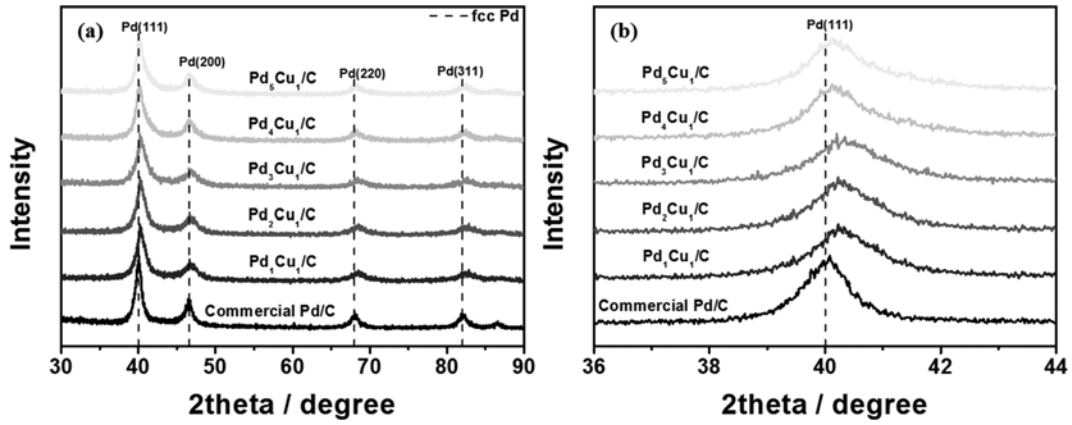

Fig. 8. XRD analysis measured in (a) full range and (b) a range of 36-44° of commercial Pd/C and Pd_xCu_y/C catalysts.

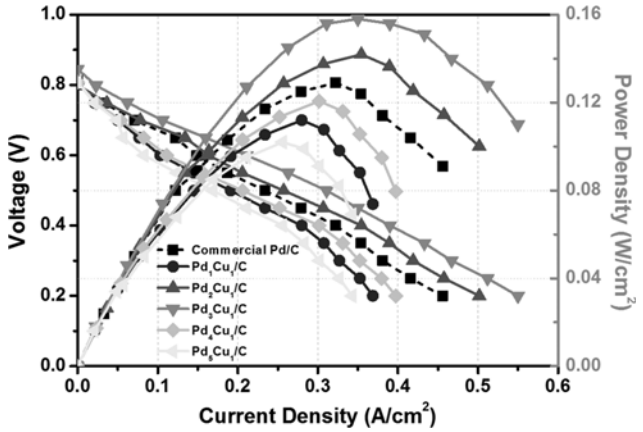

Fig. 9. Polarization curves of DFAFCs using commercial Pd/C and Pd_xCu_y/C as anodic catalysts. The curves were measured at 65 °C, while 3 M formic acid was supplied for anodic fuse with a flow rate of 10 cc min^{-1} and air was supplied for the cathode with a flow rate of 800 cc min^{-1}.

102 mW cm^{-2}, respectively. As expected, DFAFC using Pd_3Cu_1/C showed the best performance that was even 22.5% higher than DFAFC using commercial Pd/C, and the tendency about the polarization curve of DFAFC was compatible with the tendency about the reaction rate of FAOR.

CONCLUSIONS

Carbon supported PdCu bimetallic catalysts (Pd_xCu_y/Cs) were synthesized by the modified-polyol method. The ratio of Pd : Cu precursor was varied as 1 : 1, 2 : 1, 3 : 1, 4 : 1 and 5 : 1 to find a proper ratio for improving the reaction rate for FAOR, and their reaction rate data for FAOR was compared with the data in commercial Pd/C. According to the electrochemical evaluations that were incorporated by measuring their CV curves, Pd_3Cu_1/C catalyst showed the best maximum current density that was 1.68-times higher than that of commercial Pd/C catalyst.

To verify the effects of structural characteristics of Pd_xCu_y/C catalysts on the reaction rate of FAOR, various optical and spectroscopic measurements such as TEM, EDS, XPS and XRD were conducted. According to the analysis, Pd_3Cu_1/C has the particle size of 4.30 nm, which is similar to that of commercial Pd/C (4.26 nm) and a high Pd concentration, while its degree of alloying was higher than that of the others. Moreover, Pd_3Cu_1/C showed the highest positive shift of μ_p (3.5934 eV). The positive shift of μ_p induces the weakening in adsorption of COOH to Pd surface, and enhances the reaction rate of FAOR due to the accelerated desorption of O atoms that is supposed to determine the reaction rate of FAOR, confirming again that 3 : 1 (Pd : Cu) precursor ratio is the optimal to make high degree of alloying and Pd concentration in catalyst and contributed to high catalytic activity.

The polarization curve of fuel cell using Pd_3Cu_1/C was also the highest value that was 158 mW cm^{-2}, 22.5% higher than commercial Pd/C, indicating that Pd_3Cu_1/C can be used for the alternative of commercial Pd/C.

ACKNOWLEDGEMENTS

This work is supported by the Ministry of Science, ICT and Future Planning (MSIP) (No. 2016M1A2A2937143).

REFERENCES

1. K. Hansen, C. Breyer and H. Lund, *Energy*, **175**, 471 (2019).
2. S. Jain, H. Y. Chen and J. Schwank, *J. Power Sources*, **160**, 474 (2006).
3. T. E. Lipman, J. L. Edwards and D. M. Kammen, *Energy Policy*, **32**, 101 (2004).
4. C. Noh, M. Jung, D. Henkensmeier, S. W. Nam and Y. Kwon, *ACS Appl. Mater. Interfaces*, **9**, 36799 (2017).
5. H. Y. Jung, S. Jeong and Y. Kwon, *J. Electrochem. Soc.*, **163**, A5090 (2016).
6. W. Lee, C. Jo, S. Youk, J. Lee, Y. Chung and Y. Kwon, *Appl. Surf. Sci.*, **429**, 187 (2018).
7. S. Jung, L.-H. Kim, Y. Kwon and S. H. Kim, *Korean J. Chem. Eng.*, **31**, 2081 (2014).
8. K. Hyun, S. Kang and Y. Kwon, *Korean J. Chem. Eng.*, **36**, 500 (2019).
9. H. Park, K. Kim, H. Kim, D. Kim, Y. Won and S. Kim, *Korean J. Chem. Eng.*, **35**, 1547 (2018).
10. X. Cheng, Z. Shi, N. Glass, L. Zhang, J. Zhang, D. Song, Z. Liu, H.

Wang and J. Shen, *J. Power Sources*, **165**, 739 (2007).
11. T. Kim, S. Lee and H. Park, *Renew. Sustain. Energy Rev.*, **15**, 3676 (2011).
12. K. Hyun, J. H. Lee, C. W. Yoon and Y. Kwon, *Int. J. Electrochem. Sci.*, **8**, 11752 (2013).
13. S. M. Aceves, F. Espinosa-Loza, E. Ledesma-Orozco, T. O. Ross, A. H. Weisberg, T. C. Brunner and O. Kircher, *Int. J. Hydrogen Energy*, **35**, 1219 (2010).
14. T. Q. Hua, R. K. Ahluwalia, J.-K. Peng, M. Kromer, S. Lasher, K. McKenney, K. Law and K. Sinha, *Int. J. Hydrogen Energy*, **36**, 3037 (2011).
15. M. Christwardana, Y. Chung and Y. Kwon, *Korean J. Chem. Eng.*, **34**, 3009 (2017).
16. M. Christwardana, Y. Chung and Y. Kwon, *Korean J. Chem. Eng.*, **34**, 2916 (2017).
17. U. B. Demirci, *J. Power Sources*, **169**, 239 (2007).
18. Q. Weimin, D. P. Wilkinson, J. Shen, H. Wang and J. Zhang, *J. Power Sources*, **154**, 202 (2006).
19. X. Yu and P. G. Pickup, *J. Power Sources*, **182**, 124 (2008).
20. B. Hwang, S. Oh, M. Lee, D. Lee and K. Park, *Korean J. Chem. Eng.*, **35**, 2290 (2018).
21. J. Choi, K. Jeong, Y. Dong, J. Han, T. Lim, J. Lee and Y. Sung, *J. Power Sources*, **163**, 71 (2006).
22. Y. Zhu, S. Y. Ha and R. I. Masel, *J. Power Sources*, **130**, 8 (2004).
23. A. Heinzel and V. M. Barragan, *J. Power Sources*, **84**, 70 (1999).
24. S. M. Baik, J. Kim, J. Han and Y. Kwon, *Int. J. Hydrogen Energy*, **36**, 12583 (2011).
25. S. M. Baik, J. Kim, J. Han, J. Kim and Y. Kwon, *Int. J. Hydrogen Energy*, **36**, 14719 (2011).
26. S. Kim, J. Han, Y. Kwon, K.-S. Lee, T.-H. Lim, S. W. Nam and J. H. Jang, *Electrochim. Acta*, **56**, 7984 (2011).
27. Y. Kwon, S. Baek, B. Kwon, J. Kim and J. Han, *Korean J. Chem. Eng.*, **27**, 836 (2010).
28. Z. Liu, L. Hong, M. P. Tham, T. H. Lim and H. Jiang, *J. Power Sources*, **161**, 831 (2006).
29. N. Uwitonze and Y. X. Chen, *Chem. Sci. J.*, **8**, 1000167 (2017).
30. Y. Yu, Y. E. Koh, H. Lim, B. Jeong, K. Isegawa, D. Kim, K. Ueda, H. Kondoh, K. Mase, E. J. Crumlin, P. N. Jr. Ross, J. Gallet, F. Bournel and B. S. Mun, *J. Phys.: Condens. Matter*, **29**, 464001 (2017).
31. Y. Kwon, S. M. Baik, J. Han and J. Kim, *Bull. Korean Chem. Soc.*, **33**, 2539 (2012).
32. J. Cao, Z. Zhu, W. Zhao, J. Xu and Z. Chen, *Chin. J. Chem.*, **34**, 1086 (2016).
33. J. W. Hong, D. Kim, Y. W. Lee, M. Kim, S. W. Kang and S. W. Han, *Angew. Chem.*, **123**, 9038 (2011).
34. X. Xiao, H. Nam, S. H. Bhang, S. Y. Lee, J. Ahn and T. Yu, *Korean J. Chem. Eng.*, **35**, 2379 (2018).
35. M. Liao, Q. Hu, J. Zheng, Y. Li, H. Zhou, C. Zhong and B. H. Chen, *Electrochim. Acta*, **111**, 504 (2013).
36. M. A. Matin, J. Jang and Y. Kwon, *J. Power Sources*, **262**, 356 (2014).
37. S. Hu, F. Munoz, J. Noborikawa, J. Haan, L. Scudiero and S. Ha, *Appl. Catal. B*, **180**, 758 (2016).
38. S. Yang, J. Yang, Y. Chung and Y. Kwon, *Int. J. Hydrogen Energy*, **42**, 17211 (2017).
39. M. Chen, Z.-B. Wang, K. Zhou and Y.-Y. Chu, *Fuel Cells*, **10**, 1171 (2010).
40. J. A. Herron, J. Scaranto, P. Ferrin, S. Li and M. Mavrikakis, *ACS Catal.*, **4**, 4434 (2014).
41. J. Scaranto and M. Mavrikakis, *Surf. Sci.*, **650**, 111 (2016).
42. M. V. Castegnaro, A. Gorgeski, B. Balke, M. C. M. Alves and J. Morais, *Nanoscale*, **8**, 641 (2016).
43. W. P. Zhou, A. Lewera, R. Larsen, R. I. Masel, P. S. Bagus and A. Wieckowski, *J. Phys. Chem. B.*, **110**, 13393 (2006).
44. C. Xu, Y. Liu, J. Wang, H. Geng and H. Qiu, *J. Power Sources*, **199**, 124 (2012).